

Compressible Laminar Flow towards a Numerical Wind Tunnel

Ekachai Juntasaro, and Boonlue Sawatmongkhon
School of Mechanical Engineering, Institute of Engineering,
Suranaree University of Technology, Nakhon Ratchasima 30000
Phone: (6644) 224263, Fax: (6644) 224220, E-mail: junta@ccs.sut.ac.th

Abstract

The present paper is part of the research and development project on a numerical wind tunnel in which engineers can investigate the behaviour of the flow past an object of any shape. The numerical wind tunnel is one of the great challenges in the field of fluid dynamics and engineering applications because the flow can be studied at all speeds and the object of all sizes can be tested and analysed for design purposes. As the first step, the current work is carried out to develop the computer program for two-dimensional compressible laminar flow on a flat plate. The flow of this type is governed by the continuity, Navier-Stokes and energy equations, together with the equation of state. These equations are discretised and solved by using the MacCormack numerical technique that is based on the finite-difference method. The velocity and temperature distributions across the flow domain are obtained as the computed results and they are compared with the similarity solutions. It has been found that the computed results show the interaction of the shock layer with the velocity and thermal boundary layers.

1. Introduction

Fluid flow involves in many engineering applications, not only in mechanical engineering, but also in other branches of science, engineering and technology. Understanding of the flow behaviour is significant for the design and development of scientific and engineering innovations.

In fluid dynamics, the behaviour of the flow is generally governed by the continuity, Navier-Stokes and energy equations, together with the equation of state. Those governing equations can be solved either by the numerical method or by the analytical method. By the numerical method, the governing partial differential equations are discretised into a system of algebraic equations. By the analytical method, the governing equations are simplified under certain assumptions into the equation of simple form that can be readily solved.

Sophisticated computation is now possible with high-speed and large-storage computers. Thus, the computation becomes another attractive choice, apart from conventional experiments. A physical wind tunnel and highly accurate instruments for flow measurement are very expensive. As a result, the importance of the numerical wind tunnel is underlined as an alternative way to study the flow behaviour effectively and economically. As a long-term research and development project, this

numerical wind tunnel is aimed to be able to simulate the internal and external flows at all speeds. For internal flow, the cross-sectional area of the numerical tunnel can be made to any shape to suit the applications. The effects of the external flow on the object of any shape can be investigated when it is placed within the numerical tunnel.

Unlike the physical wind tunnel, any kind of fluids can be studied within this numerical tunnel since there is no limitation of study in any dangerous situation. One of those circumstances is when the fluid is contaminated by radioactivity or dangerous substances. This is the motivation of the present work to develop a numerical wind tunnel. The first step of the development is to simulate steady compressible laminar flow on a flat plate.

2. Governing Equations

Compressible flow is governed by the continuity, Navier-Stokes and energy equations, together with the equation of state. For two-dimensional flow, the governing equations can be written in terms of tensor notation (where $i = 1$ and 2 , corresponding to x and y directions respectively) as follows:

Continuity equation

$$\frac{\partial \rho}{\partial t} + \frac{\partial(\rho u_i)}{\partial x_i} = 0 \quad (1)$$

where ρ is the fluid density and u_i is the flow velocities.

Navier-Stokes equations

$$\frac{\partial(\rho u_i)}{\partial t} + \frac{\partial(\rho u_i u_j)}{\partial x_j} = -\frac{\partial p}{\partial x_i} + \frac{\partial \tau_{ij}}{\partial x_j} \quad (2)$$

where p is the pressure and τ_{ij} is the stresses which can be defined as:

$$\tau_{ij} = -\frac{2}{3}\mu\delta_{ij}\frac{\partial u_k}{\partial x_k} + \mu\left(\frac{\partial u_i}{\partial x_j} + \frac{\partial u_j}{\partial x_i}\right) \quad (3)$$

where μ is the fluid viscosity and δ_{ij} is the Kronecker delta: $\delta_{ij} = 0$ for $i \neq j$ and $\delta_{ij} = 1$ for $i = j$.

Energy equation

$$\frac{\partial(\rho e_t)}{\partial t} + \frac{\partial(\rho e_t u_j)}{\partial x_j} = -\frac{\partial(p u_j)}{\partial x_j} - \frac{\partial q_j}{\partial x_j} + \frac{\partial(u_j \tau_{ij})}{\partial x_i} \quad (4)$$

where e_t is the total energy of the flow which is defined in terms of the internal energy, e , and the kinetic energy as:

$$e_t = e + \frac{1}{2}(u^2 + v^2) \quad (5)$$

and q_j is the heat flux which is defined by Fourier's law of heat conduction as:

$$q_j = -k \frac{\partial T}{\partial x_j} \quad (6)$$

where T is the temperature of the flow and k is the thermal conductivity of the fluid. For the calorically perfect gas, the internal energy can be defined as:

$$e = c_v T \quad (7)$$

where c_v is the specific heat at constant volume.

Equation of state

$$p = \rho R T \quad (8)$$

where R is the gas constant.

With the above five equations, Equations (1), (2), (4) and (8), there appear five dependent variables, that is, ρ , u , v , p and T so that this system of equations has the closed form. However, the fluid properties, μ and k , in the compressible flow are changed as the temperature varies so that they must be defined in terms of temperature by the following relations:

Sutherland's law

$$\mu = \mu_\infty \left(\frac{T}{T_\infty} \right)^{3/2} \frac{T_\infty + 110}{T + 110} \quad (9)$$

where μ_∞ and T_∞ are the viscosity and temperature at standard sea level conditions respectively.

Prandtl number

$$Pr = \frac{\mu c_p}{k} \quad (10)$$

where c_p is the specific heat at constant pressure.

3. Numerical Method

The governing equations can be expressed in vector notation for simplicity as follows:

$$\frac{\partial U}{\partial t} + \frac{\partial E}{\partial x} + \frac{\partial F}{\partial y} = 0 \quad (11)$$

where U is the solution vector, and E and F are the x - and y -flux vectors respectively as follows:

$$U = [\rho \quad \rho u \quad \rho v \quad \rho e_t]^T \quad (12)$$

$$E = \begin{bmatrix} \rho u \\ \rho u u + p - \tau_{xx} \\ \rho v u - \tau_{xy} \\ \rho e_t u + p u + q_x - \tau_{xx} u - \tau_{xy} v \end{bmatrix} \quad (13)$$

$$F = \begin{bmatrix} \rho v \\ \rho u v - \tau_{xy} \\ \rho v v + p - \tau_{yy} \\ \rho e_t v + p v + q_y - \tau_{xy} u - \tau_{yy} v \end{bmatrix} \quad (14)$$

The governing equations can be solved numerically by the finite difference method. In the present work, the MacCormack technique is employed to discretise the governing partial differential equations into the finite difference equations. Using a Taylor series expansion, the solution vector at grid point (i,j) and time $t + \Delta t$ can be expressed about that at grid point (i,j) and time t as:

$$U_{i,j}^{t+\Delta t} = U_{i,j}^t + \left(\frac{\partial U}{\partial t} \right)_{av} \Delta t \quad (15)$$

where

$$\left(\frac{\partial U}{\partial t} \right)_{av} = \frac{1}{2} \left[\left(\frac{\partial U}{\partial t} \right)_{i,j}^t + \left(\frac{\partial U}{\partial t} \right)_{i,j}^{t+\Delta t} \right] \quad (16)$$

Equation (16) is calculated by the following two steps:

Predictor step

$\bar{U}_{i,j}^{t+\Delta t}$ is predicted by using a Taylor series expansion of $\bar{U}_{i,j}^{t+\Delta t}$ about $U_{i,j}^t$:

$$\bar{U}_{i,j}^{t+\Delta t} = U_{i,j}^t + \left(\frac{\partial U}{\partial t} \right)_{i,j}^t \Delta t \quad (17)$$

where $\left(\frac{\partial U}{\partial t} \right)_{i,j}^t$ is evaluated from Equation (11) by using the forward difference for spatial derivatives:

$$\left(\frac{\partial U}{\partial t} \right)_{i,j}^t = -\frac{E_{i+1,j}^t - E_{i,j}^t}{\Delta x} - \frac{F_{i,j+1}^t - F_{i,j}^t}{\Delta y} \quad (18)$$

Corrector step

$\left(\frac{\partial U}{\partial t} \right)_{i,j}^{t+\Delta t}$ is determined from Equation (11) by

using the backward difference for spatial derivatives:

$$\left(\frac{\partial U}{\partial t} \right)_{i,j}^{t+\Delta t} = -\frac{\bar{E}_{i,j}^{t+\Delta t} - \bar{E}_{i-1,j}^{t+\Delta t}}{\Delta x} - \frac{\bar{F}_{i,j}^{t+\Delta t} - \bar{F}_{i,j-1}^{t+\Delta t}}{\Delta y} \quad (19)$$

where $\bar{E}_{i,j}^{t+\Delta t}$ and $\bar{F}_{i,j}^{t+\Delta t}$ are calculated by using $\bar{U}_{i,j}^{t+\Delta t}$. Then, Equations (18) and (19) are used to calculate $\left(\frac{\partial U}{\partial t} \right)_{i,j}^{t+\Delta t}$. Finally, $U_{i,j}^{t+\Delta t}$ is corrected by Equation (15).

Calculations of $U_{i,j}^{t+\Delta t}$ are made repeatedly until the flow reaches the steady state where the dependent variables no longer vary with time.

4. Similarity Method

The governing equations can be solved by the similarity method. The idea of this method is to define appropriate variables to reduce the number of governing equations and then define similarity variables to transform the partial differential equations to the ordinary differential equations. For the current work, the Illingworth transformation is adopted to solve the governing equations of steady compressible boundary layers on a flat plate where the streamwise pressure gradient is equal to zero.

The stream function $\psi(x, y)$ for compressible flow can be defined as:

$$\frac{\partial \psi}{\partial y} = \rho u \quad (20)$$

$$\frac{\partial \psi}{\partial x} = -\rho v \quad (21)$$

By the definition of the stream function, the continuity equation can be eliminated.

The similarity variables (ξ, η) can be defined as

$$\xi(x) = \int_0^x \rho_\infty(x) U_\infty(x) \mu_\infty(x) dx \quad (22)$$

$$\eta(x, y) = \frac{U_\infty(x)}{\sqrt{2\xi(x)}} \int_0^y \rho dy \quad (23)$$

where the subscript ∞ denotes the freestream. Using these similarity variables, the x-component of the Navier-Stokes equations can be transformed to the following ordinary differential equation:

$$(Cf'')' + ff'' = 0 \quad (24)$$

where f is the transformed function and depends on η only, and C is the Chapman-Rubensin parameter which is expressed as:

$$C = \frac{\rho \mu}{\rho_\infty \mu_\infty} \quad (25)$$

Using the equation of state and Sutherland's law, C can be expressed in terms of temperature as:

$$C = \left(\frac{T}{T_\infty} \right)^{1/2} \left(\frac{T_\infty + 110}{T + 110} \right) \quad (26)$$

The value of C can be obtained at a reference temperature T^* , that is, $C \equiv C^*$ where T^* is defined by the empirical Eckert correlation:

$$\frac{T^*}{T_\infty} \approx 0.5 + 0.039M_\infty^2 + 0.5 \frac{T_w}{T_\infty} \quad (27)$$

where M_∞ is the freestream Mach number and T_w is the wall temperature. Thus, Equation (24) can be simplified to

$$C^* f''' + ff'' = 0 \quad (28)$$

with the following boundary conditions:

$$f(0) = 0 \quad (29)$$

$$f'(0) = 0 \quad (30)$$

$$f'(\infty) = 1 \quad (31)$$

For boundary layers, the y-component of the Navier-Stokes equations is simply reduced to a zero cross-stream pressure gradient. Since the energy equation is coupled to the x-component of the Navier-Stokes equations, the temperature-velocity, or Crocco-Busemann, relation is employed to determine the temperature distribution:

$$\frac{T}{T_\infty} = 1 + r \left(\frac{\gamma - 1}{2} \right) M_\infty^2 \left[1 - \frac{u^2}{U_\infty^2} \right] + \left(\frac{T_w - T_{aw}}{T_\infty} \right) \left[1 - \frac{u}{U_\infty} \right] \quad (32)$$

where γ is the specific-heat ratio, r is the recovery factor defined as:

$$r = \sqrt{\text{Pr}} \quad \text{for laminar flow} \quad (33)$$

and T_{aw} is the adiabatic wall temperature defined as:

$$T_{aw} = T_\infty \left[1 + r \left(\frac{\gamma - 1}{2} \right) M_\infty^2 \right] \quad (34)$$

5. Results and Discussion

Steady compressible laminar boundary layers on a flat plate are studied at three freestream Mach numbers: $M_\infty = 2, 4$ and 6 . Flow conditions are summarised in Table 1.

Table 1 Flow conditions

Physical Parameter	Value or Type
Plate length (L)	0.01 mm
Fluid	Air
γ	1.4
Pr	0.71
R	287 J/kg.K
c_p	1005 J/kg.K
T_∞	288.16 K
p_∞	101325 Pa
ρ_∞	1.23 kg/m ³
μ_∞	1.79×10^{-5} kg/m.s
T_w	T_∞

The height of the computational domain is specified by

$$H = 5 \left(\frac{5L}{\sqrt{\rho_\infty U_\infty L / \mu_\infty}} \right) \quad (35)$$

The mean free path of a gas can be estimated by the following expression:

$$\ell = 1.26 \frac{\mu}{\rho \sqrt{RT}} \quad (36)$$

which is recommended by White (1999). With the freestream condition in Table 1, the mean free path of air is equal to 6.4×10^{-8} which is very small compared with the computational domain $L \times H$. Thus, the treatment of air as a continuum is valid here.

The numerical solutions have been carried out by using 20×20 , 40×40 and 80×80 grid points. The 40×40 solutions are considered as grid-independent results because the difference between 40×40 and 80×80 ones is so small.

The size of the time step is suggested by MacCormack (1988) as:

$$\Delta t = \min[C(\Delta t)_{i,j}] \quad (37)$$

where C is the Courant number ($0.5 \leq C \leq 0.8$) and $(\Delta t)_{i,j}$ is the local size of the time step at grid point (i,j) defined as:

$$(\Delta t)_{i,j} = \left[\frac{|u_{i,j}|}{\Delta x} + \frac{|v_{i,j}|}{\Delta y} + c_{i,j} \sqrt{\frac{1}{\Delta x^2} + \frac{1}{\Delta y^2}} + 2v'_{i,j} \left(\frac{1}{\Delta x^2} + \frac{1}{\Delta y^2} \right) \right]^{-1} \quad (38)$$

where $u_{i,j}$, $v_{i,j}$ and $c_{i,j} = \sqrt{\gamma RT_{i,j}}$ are the local values of the streamwise and cross-stream velocities and the speed of sound at grid point (i,j) respectively and $v'_{i,j}$ is defined as:

$$v'_{i,j} = \max \left[\frac{\frac{4}{3} \mu_{i,j} \left(\frac{\gamma \mu_{i,j}}{\text{Pr}} \right)}{\rho_{i,j}} \right] \quad (39)$$

where $\rho_{i,j}$ and $\mu_{i,j}$ are the local density and viscosity of the fluid at grid point (i,j) respectively. For the present numerical solution, the Courant number is taken as 0.6.

Initial conditions are specified by the freestream values and boundary conditions are specified as follows:

At the leading edge of the plate or at grid point (1,1):

$$\begin{aligned} u_{1,1} &= v_{1,1} = 0 \\ T_{1,1} &= T_\infty \\ p_{1,1} &= p_\infty \end{aligned}$$

At the plate, or at grid points (i,1), except grid point (1,1):

$$\begin{aligned} u_{i,1} &= v_{i,1} = 0 \\ T_{i,1} &= T_w \\ p_{i,1} &= 2p_{i,2} - p_{i,3} \end{aligned}$$

At the inlet or at grid points (1,j), except grid point (1,1):

$$\begin{aligned} u_{1,j} &= U_\infty \\ v_{1,j} &= 0 \\ T_{1,j} &= T_\infty \\ p_{1,j} &= p_\infty \end{aligned}$$

At the outlet or at grid points (imax,j), except grid points (imax,1) and (imax,jmax):

$$\begin{aligned} u_{i \max} &= 2u_{i \max-1,j} - u_{i \max-2,j} \\ v_{i \max} &= 2v_{i \max-1,j} - v_{i \max-2,j} \\ T_{i \max} &= 2T_{i \max-1,j} - T_{i \max-2,j} \\ p_{i \max} &= 2p_{i \max-1,j} - p_{i \max-2,j} \end{aligned}$$

At the upper boundary of the computational domain:

$$\frac{\partial u}{\partial y} = \frac{\partial v}{\partial y} = \frac{\partial T}{\partial y} = \frac{\partial p}{\partial y} = 0$$

The fluid density at the boundaries of the computational domain can be calculated from the equation of state.

The converged solutions are obtained when the density at each grid point changes less than 10^{-8} between time steps. The distributions of the streamwise velocity and temperature across the flow at the trailing edge of the plate are plotted for analysis where the

normalised streamwise velocity is $\frac{u}{U_\infty}$, the normalised

temperature is $\frac{T}{T_\infty}$ and the normalised cross-stream distance $\frac{y}{\sqrt{x\mu_\infty/\rho_\infty U_\infty}}$.

The computed results of the streamwise velocity at freestream Mach numbers $M_\infty = 2, 4$ and 6 are shown in Figures 1, 2 and 3 respectively in which they are compared with the similarity solutions at corresponding Mach numbers. It is found that the trends between the computed results and the similarity solutions are similar except that the shock can be captured by the numerical method while the similarity method cannot.

As the Mach number increases, the numerical solutions show that the shock layer becomes thinner while the similarity solutions demonstrate that the velocity boundary layer is thicker.

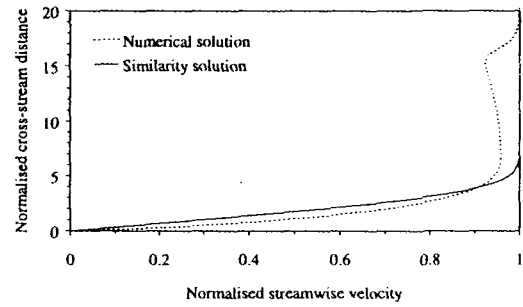


Figure 1 Velocity distributions at $M_\infty = 2$

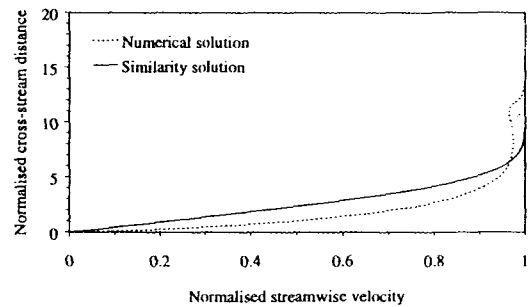


Figure 2 Velocity distributions at $M_\infty = 4$

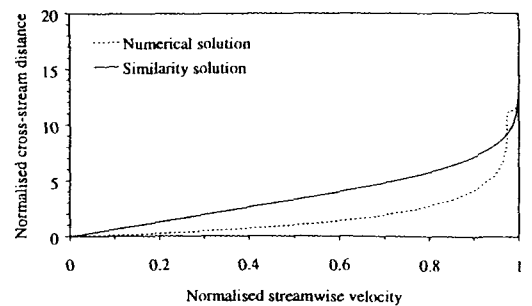


Figure 3 Velocity distributions at $M_\infty = 6$

The computed results of the temperature at freestream Mach numbers $M_\infty = 2, 4$ and 6 are illustrated in Figures 4, 5 and 6 respectively in which they are compared with the similarity solutions at corresponding Mach numbers. Both the computed results and the similarity solutions show almost the same peak of the temperature near the wall. As found in the velocity distributions, the shock is also observed in the numerical solutions of the temperature.

As the Mach number increases, a decrease in the thickness of the shock layer is found in the numerical solutions whereas an increase in the thickness of the thermal boundary layer is detected in the similarity solutions.

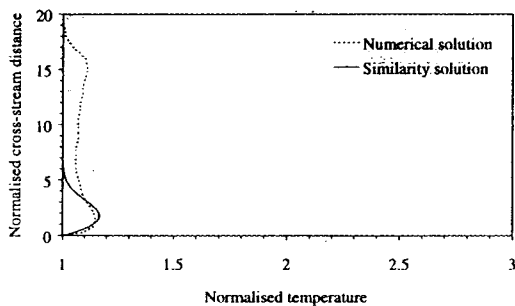


Figure 4 Temperature distributions at $M_\infty = 2$

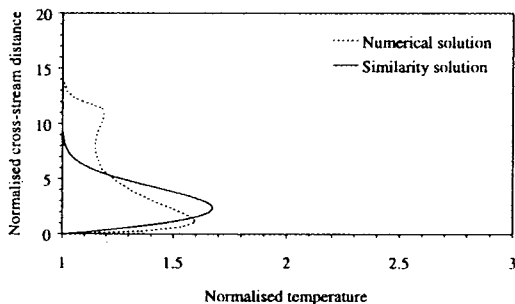


Figure 5 Temperature distributions at $M_\infty = 4$

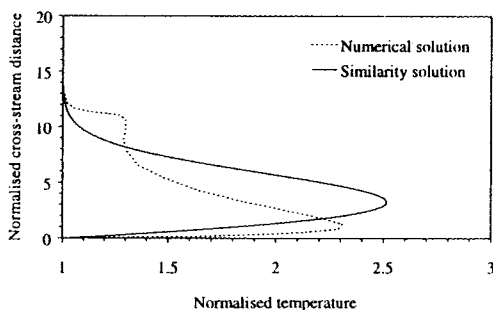


Figure 6 Temperature distributions at $M_\infty = 6$

6. Conclusions

Both numerical and similarity solutions of the compressible laminar flow on a flat plate are presented in the present paper. The numerical method is capable of capturing the shock occurring in the flow while the

similarity method cannot. The shock forms the layer along the plate leading to an interaction of the shock layer with the velocity and thermal boundary layers. This interaction becomes more obvious when the numerical solutions are compared with the similarity solutions where there exist only the velocity and thermal boundary layers with no shock. It has been found in the numerical solutions that the shock causes the velocity and thermal boundary layers thicker as the Mach number is decreased from 6 to 2.

References

- [1] Anderson, J.D., Jr. (1995) "Computational Fluid Dynamics: The Basics with Applications," McGraw-Hill.
- [2] Hoffman, J.D. (1992) "Numerical Methods for Engineers and Scientists," McGraw-Hill.
- [3] MacCormack, R.W. (1988) "Current Status of Numerical Solutions of the Navier-Stokes Equations," AIAA paper 88-0513.
- [4] Schlichting, H. (1979) "Boundary-Layer Theory," 7th edition, McGraw-Hill.
- [5] White, F.M. (1991) "Viscous Fluid Flow," 2nd edition, McGraw-Hill.
- [6] White, F.M. (1999) "Fluid Mechanics," 4th edition, McGraw-Hill.